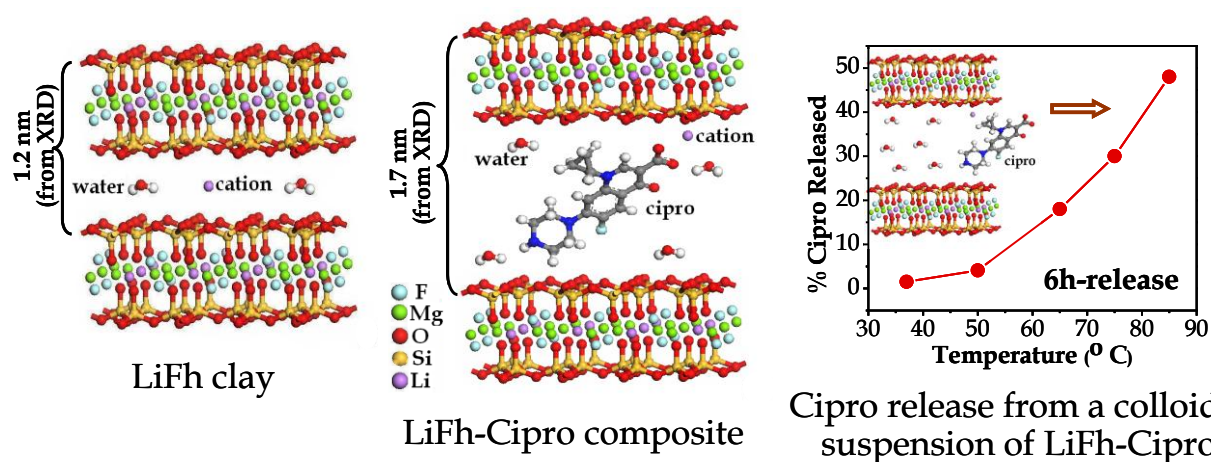


## Smectite Clay as Ciprofloxacin Delivery System: Intercalation and Temperature Controlled Release Properties

A. Rivera, L. Valdés, J. Jiménez, I. Pérez, A. Lam, E. Altshuler, L. C. de Ménorval,  
J. O. Fossum, E. L. Hansen, Z. Rozynek

Ciprofloxacin (Cipro) incorporation into Li-fluorhectorite (LiFh) clay and its temperature-controlled release.



Cipro release from a colloidal suspension of LiFh-Cipro

### **Highlights of the article**

- Successful intercalation of ciprofloxacin into a smectite clay (Li-fluorohectorite) with potential pharmaceutical and biomedical applications.
- Structural characterization of the raw material and the clay-drug composites.
- Demonstration of the temperature-controlled drug release abilities of a colloidal suspension of the clay-drug composite, following pharmaceutical standards.

**Smectite Clay as Ciprofloxacin Delivery System:  
Intercalation and Temperature Controlled Release Properties**

**A. Rivera<sup>1\*</sup>, L. Valdés<sup>2</sup>, J. Jiménez<sup>3</sup>, I. Pérez<sup>4</sup>, A. Lam<sup>1</sup>, E. Altshuler<sup>5</sup>, L. C. de Ménorval<sup>6</sup>,  
J. O. Fossum<sup>7\*</sup>, E. L. Hansen<sup>7†</sup>, Z. Rozynek<sup>7‡</sup>**

<sup>1</sup>*Zeolites Engineering Laboratory, Institute of Materials Science and Technology (IMRE),  
University of Havana, Cuba;*

<sup>2</sup>*Department of Basic Chemistry, Institute of Pharmacy and Food (IFAL),  
University of Havana, Cuba;*

<sup>3</sup>*University Laboratory of Characterization of the Structure of the Substance, (LUCES),  
Institute of Materials Science and Technology (IMRE),  
University of Havana, Cuba*

<sup>4</sup>*Department of Drugs Technology and Control, Institute of Pharmacy and Food (IFAL);  
University of Havana, Cuba;*

<sup>5</sup>*Superconductivity Laboratory and “Henri Poincaré” Group of Complex Systems, Physics  
Faculty, University of Havana, Cuba;*

<sup>6</sup>*Institut Charles Gerhardt Montpellier, Equipe Agregats, Interface, et Matériaux pour l'Energie  
(AIME), Université Montpellier 2, France;*

<sup>7</sup>*Department of Physics, Norwegian University of Science and Technology (NTNU),  
Trondheim, Norway*

---

\* Corresponding authors: e-mail: [aramis@imre.oc.uh.cu](mailto:aramis@imre.oc.uh.cu), [jon.fossum@ntnu.no](mailto:jon.fossum@ntnu.no)

† Present address: Department of Monitoring and Research, Norwegian Radiation Protection Authority, Oslo, Norway

‡ Present address: Institute of Physical Chemistry, Polish Academy of Sciences, Warsaw, Poland

## **Abstract**

Clays have shown to be good candidates as drug delivery carriers. In the present paper, we use the temperature-dependent swelling of smectite clays to produce clay-drug composites with sizable drug load capacity. Specifically, we obtain a fluorohectorite-ciprofloxacin (Fh-Cipro) composite, in which a true intercalation of the drug between the clay interlayers has been verified by various experimental techniques. We evaluate the thermally activated drug release from a colloidal suspension of nanosized composite particles in water as well as in synthetic gastric juice from 37<sup>0</sup>C (body temperature) to 85<sup>0</sup>C. The temporal profiles of drug release from the clay fulfil the pharmaceutical standards for these systems. In this work, we have been able to produce a clay-based Temperature Controlled Release System (TCRS) with potential biomedical applications.

Keywords: drug, antibiotic, smectite, fluorohectorite, clay

## 1. Introduction

Temperature-controlled drug release is desirable in many scenarios: for example, when the local body temperature varies during different stages of a disease, or in response to external stimuli. To date, just a few materials able to release an active principle as a function of temperature have been investigated. In recent years, hydrogel-based composites have been created to release proteins [1,2], as well as microscale polymers able to release small molecules and nanoparticles within a certain temperature range [3].

In the last years, different porous materials have been used as drug hosts [4,5]. Among clay minerals, montmorillonite is the most commonly used for drug delivery applications [6,7], although kaolin and laponite have been also investigated [8]. Most of them have been typically used as hosts for pH-controlled release.

Synthetic hectorites show a number of advantages as drug hosts, like controllable pore size distribution, purity and composition, which result in higher reproducibility. In addition, these materials have been shown to be non-toxic for trans-dermal application and oral administration [5,9]. Their swelling transition [10], on the other hand, suggests their potential as hosts of large molecules of pharmaceutical interest and their temperature controlled release. However, few reports about the use of fluorohectorite, a commercially available synthetic smectite, as a drug hosting material, can be found in the literature [5,6,11]. From the structural point of view, in their dry form, the layers assemble to form stack-of-card like particles. Figure 1a shows the atomic structure of lithium fluorohectorite (LiFh) clay. The stacks are held together by van der Waals forces, and by electrostatic forces in the case of clays with negative layer charges. In the interlayer space of these clays there are positive counter-ions, leading to an attractive interaction similar to a salt bridge [12,13], and they can also take up water between lamellae [14,15].

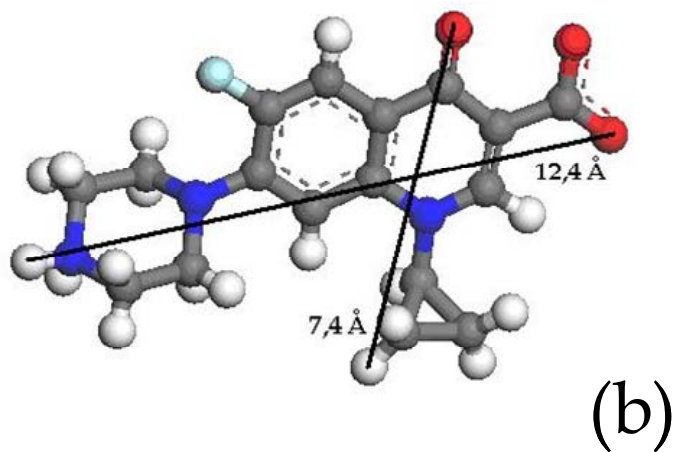
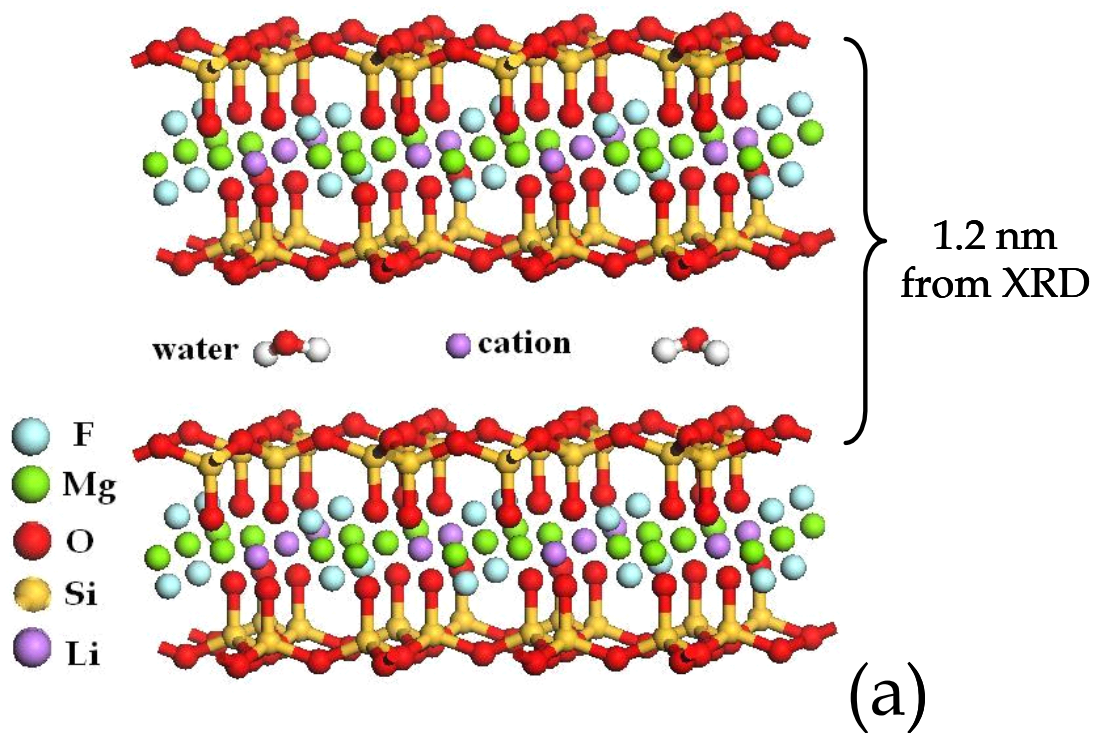


**Figure 1.** Schematic representation of the atomic (a) and molecular structure (b) of the LiFh clay and ciprofloxacin drug, respectively.

In order to take advantage of the temperature-dependent swelling property of these materials, we attempted to incorporate drugs with molecular dimensions of the order of the

interlayer space reached when the clay is thermally activated, and different structural features. In the present work, we have successfully incorporated the antibiotic ciprofloxacin (a broadspectrum antibacterial agent for oral administration used to treat various bacterial infections) into a Li-fluorohectorite (LiFh). Figure 1b illustrates the Cipro molecular structure. X ray diffraction (XRD) data suggests a true intercalation of the drug molecules between the clay layers. In addition, thermogravimetric analysis was performed as a complementary method, and the obtained results confirm the observation from the scattering data. We have also investigated the release of the drug molecules from the colloidal clay suspension, which shows a temperature-controlled release of the drug. The release profiles meet the pharmaceutical standards for these kinds of systems. We will call the obtained composites *Temperature Controlled Release Systems* (TCRS).

## 2. Material and methods

### 2.1 Sample preparation and characterization

#### *Sample preparation*

The chemical composition of fluorohectorite synthetic 2:1 smectite clay is  $M_x(Mg_{6-x}Li_x)F_4Si_8O_{20}$ , where M denotes the exchangeable cations. These clay particles are polydisperse with lateral dimensions of the order of  $\mu m$  and they possess a net negative surface charge ( $x e^-$  per unit cell), which is balanced by counter ions localized between clay lamellar sheets. Ideally  $x = 1.2$  [16].

We purchased Li-fluorohectorite (LiFh) from Corning Inc., New York, which we characterized by X-ray diffraction (XRD) and Atomic Absorption Spectrometry (AAS) using the procedures described in the next section. From those studies we conclude that the purchased

material contains about 80% by mass of LiFh clay with nominal formula  $\text{Li}_x(\text{Mg}_{6-x}\text{Li}_x)\text{Si}_8\text{O}_{20}\text{F}_4$  with  $x = 1.2$ , and about 20% of  $\text{Li}_2\text{O}\cdot 2\text{SiO}_2$  impurities.

Two different modified forms, Na-fluorohectorite (Na-Fh) and Cu-fluorohectorite (Cu-Fh) were prepared according to the ionic exchange procedure described in [17]. Ciprofloxacin hydrochloride, acetaminophen and ibuprofen —pharmaceutical-grade according to Pharmacopoeia [18]— were the model drugs studied; and they were used as received from the Cuban pharmaceutical industry.

For the interactions, 50 ml of drug solutions at 3 mg/ml (pH near 4.5) were put in contact with 0.5 g of each clay, resulting in a colloidal suspension. The experiments were carried out at room temperature and at  $65^\circ\text{C} \pm 5^\circ\text{C}$  during 4 h and 24 h, in order to study the influence of temperature and time on the amount of drug captured by the clays. All these studies took place under agitation with a magnetic stirrer. By the end of the interactions, the pH of the Cipro-clay suspensions was around 8. In the case of drug adsorption in the suspensions, the drugs concentrations before and after the contact with the clays were analyzed and quantified by ultraviolet spectroscopy (UV), according to standard procedures [18] (the drug-clay suspensions were centrifuged, and the drug contents in the supernatant was determined by UV relative to calibration curves for the pure drug solutions). The UV spectra were collected by means of a Rayleigh UV-2601 spectrophotometer in the wavelength interval 200-400 nm (including the adsorption maxima at 276, 245 and 273 nm for the ciprofloxacin, acetaminophen and ibuprofen, respectively). Each composite LiFh-Cipro, NaFh-Cipro and CuFh-Cipro was prepared in several batches, in order to check repeatability. As demonstrated below, the UV studies show that, among the drugs investigated, only Cipro is significantly captured by the clay, so further characterization was performed only on Cipro-clay composites.



### *Characterization*

Each Cipro-clay suspension was centrifuged, and the resulting supernatant fluid was analyzed by means of atomic absorption spectroscopy to determine the ionic contents. A PYE UNICAM SP9 atomic absorption spectrophotometer was employed.

The X-ray diffraction (XRD), for the different clays before and after the drug sorption, were conducted at a Philips Xpert diffractometer, using Cu K $\alpha$  radiation ( $\lambda = 1.54 \text{ \AA}$ ). The  $2\theta$  range was from 2 to 40°.

The solid clay samples were analyzed by Thermal Gravimetric Analysis (TGA) and Infrared Spectroscopy (IR) before and after interaction with the Cipro. TGA was performed on a NETZSCH STA 409 PC/PG thermal analyzer under dry air flow (50 ml/min), and a heating rate of 10°C/min, from 20 up to 800 °C. The sensitivity of the thermobalance is  $\pm 1 \text{ }\mu\text{g}$ . To perform IR analysis, the solids were dried overnight in an oven at 100°C and 65°C for the native clay and the clays-drug composites, respectively (the lower temperature used in the case of the composite avoids Cipro decomposition). A Nicolet AVATAR 330 Fourier-transform IR spectrometer, in the wavenumber interval 400-4000  $\text{cm}^{-1}$ , was used. The samples were prepared using the KBr pressed-disk technique, with 0.8% inclusion of the material to be analyzed.

### *2.3 Drug release*

The studies of Cipro release from the composites were carried out for LiFh clay. Colloidal suspensions were obtained by putting in contact approximately 30 mg of the powdered composite (equivalent to 8.3 mg of ciprofloxacin determined by UV as described before) with 50 ml of synthetic gastric juice without pepsine at  $37 \pm 1^\circ\text{C}$  —according to the method reported in the Pharmacopoeia for this kind of systems [18], and 100 rpm stirring. Release studies under identical conditions but at  $65 \pm 5^\circ\text{C}$  were also carried out in order to evaluate the temperature

dependence of the Cipro release from clay. For both temperatures, aliquots of the solutions were collected at scheduled intervals and centrifuged. Each time, the supernatant was removed and replaced with 2 ml of synthetic gastric juice. The drug concentration in the solution as a function of time was measured by UV spectroscopy. The experiments were made in triplicate and the average values are reported.

### **3. Results and Discussion**

#### *3.1 Drug intercalation*

The UV measurements demonstrated that, among the three drugs investigated, only Cipro shows a significant affinity with the LiFh clay. No clay–drug interaction could be detected in the case of acetaminophen and ibuprofen under the conditions described above.

When sampled by UV at 4 h and 24 h, the same amount of drug incorporation was measured (277 mg of Cipro per gram of clay; equivalent to 8.3 mg of Cipro per 30 mg of composite). Thus, in the following we use 4 h as the sorption time for our samples.

We also tested Na-Fh and Cu-Fh, and we observed that the former was able to incorporate Cipro, while the latter was not, under the present experimental conditions. But in the present study we will only concentrate on LiFh.

#### *3.2 Chemical and physical characterization of samples*

For Atomic Absorption Spectrometry (AAS) measurements, 0.1 g of LiFh was digested overnight using HCl, HF and HClO<sub>4</sub> in 100 ml of water. After that, the dissolutions were analyzed by mean of standard AAS (PYE UNICAM SP9). The whole process was replicated five times resulting in a half unit cell chemical formula  $\text{Li}_x(\text{Mg}_{6-x}\text{Li}_x)\text{Si}_8\text{O}_{20}\text{F}_4$  with  $x = 1.2$  for the clay

phase (80% by weight of the sample powder), and  $\text{Li}_2\text{O}\cdot 2\text{SiO}_2$  for the impurities (20 % by weight of the sample powder).

The XRD characterization confirmed the presence of  $\text{Li}_2\text{O}\cdot 2\text{SiO}_2$  impurities, and that they were not involved in the Cipro capture, since its main Bragg peaks [19] did not show any shifts in positions after contact with the Cipro solution. Using XRD we studied (001) Bragg scattering from the clay stacks. Figure 2 shows the diffraction patterns for LiFh and LiFh-Cipro composite. In the case of the native LiFh sample there is one layer of water intercalated in the stacks in ambient conditions (peak marked as (a) in the figure) [20]. The LiFh-Cipro samples under study were prepared as described above (4h interaction and pH near 8). The XRD pattern for LiFh-Cipro shows four peaks marked as b-e in the figure. Peak (b) is likely due to clay stacks in the composite that only have two layers of water intercalated [20]. Peak (c) represents clay stacks with Cipro intercalated (Cipro is a much larger molecule than water and produces a much larger d-spacing increase). Peaks (d) and (e) most likely correspond to one and two layers of water intercalated in addition to the Cipro, respectively. A sketch of the atomic structure of LiFh with intercalated Cipro is shown in Figure 3.

IR transmittance spectra for Cipro, LiFh and the LiFh-Cipro composite are shown in Fig. 4. The characteristic O—H and Si—O bands of the LiFh sample are assigned in the spectrum (see Fig. 4b): The main Si—O stretching band in-plane at  $997\text{ cm}^{-1}$  and the Si—O out-of-plane bending band at  $710\text{ cm}^{-1}$ , as well as the Si—O in-plane bending band at  $472\text{ cm}^{-1}$  were observed. In addition we also observed the Si—O stretching out-of-plane at  $1086\text{ cm}^{-1}$  [21]. In the Cipro spectrum, the most characteristic bands are those in the interval of 1800-1200. The band at  $1707\text{ cm}^{-1}$  is ascribed to the carboxylic acid C=O stretching, that of  $1624\text{ cm}^{-1}$  to the C=O stretching

for ketone, and the band at  $1271\text{ cm}^{-1}$  for the coupling of the carboxylic acid C—O stretching and O—H deformation [22-24].

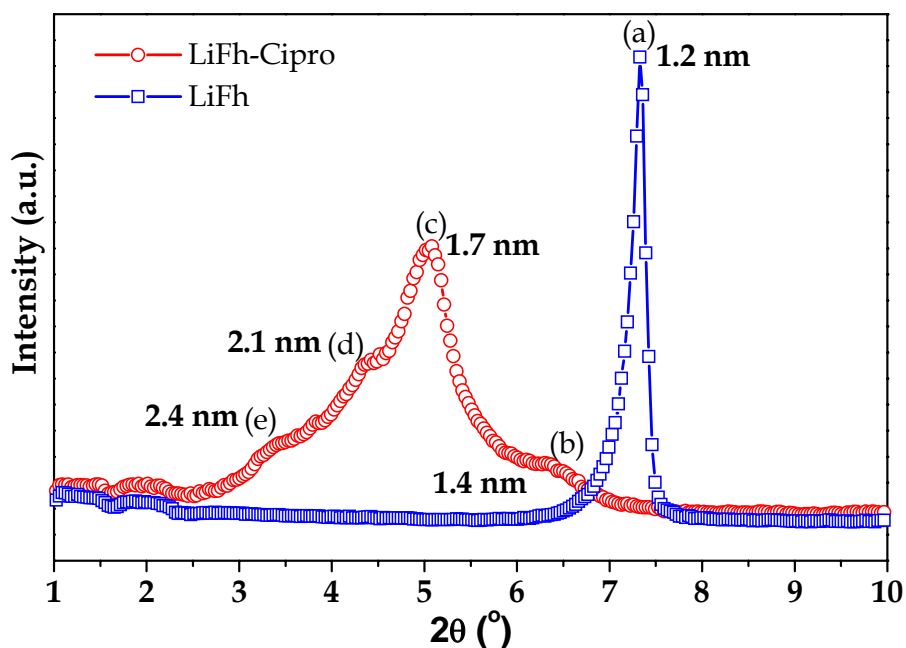


**Figure 2.** Diffraction patterns for LiFh and LiFh-Cipro composite.

The band at  $1707\text{ cm}^{-1}$  disappears in the composite LiFh-Cipro spectrum. A possible explanation of this is as follows: The natural pH of a pure Cipro solution and the natural pH of the pure clay in aqueous suspension measured by us is about 4.5 and 10, respectively. We also measure the pH of the Cipro-clay suspension to be around 8. This high pH value leads to de-protonation of the carboxylic group, which results in the C=O bond becoming two more or less equivalent C—O bonds. Therefore, the peak corresponding to —COOH disappears from the LiFh-Cipro spectrum, and is replaced by two peaks at  $1581\text{ cm}^{-1}$  and  $1390\text{ cm}^{-1}$ , which may be assigned to asymmetric ( $\nu_{\text{as}}\text{COO}^-$ ) and symmetric ( $\nu_{\text{s}}\text{COO}^-$ ) stretching vibrations of the —COO<sup>-</sup> group, respectively. This is attributed to the existence of the ciprofloxacin in zwitterionic form, where the COO<sup>-</sup> group is deprotonated and the piperazinyl group is protonated [25,26]. In addition, due to the

COOH group deprotonation and loss of the carboxylic acid C=O stretching, a significant decrease in intensity the coupled COOH modes at  $1271\text{ cm}^{-1}$  was also observed. This behaviour has been observed previously in similar systems [23,27].

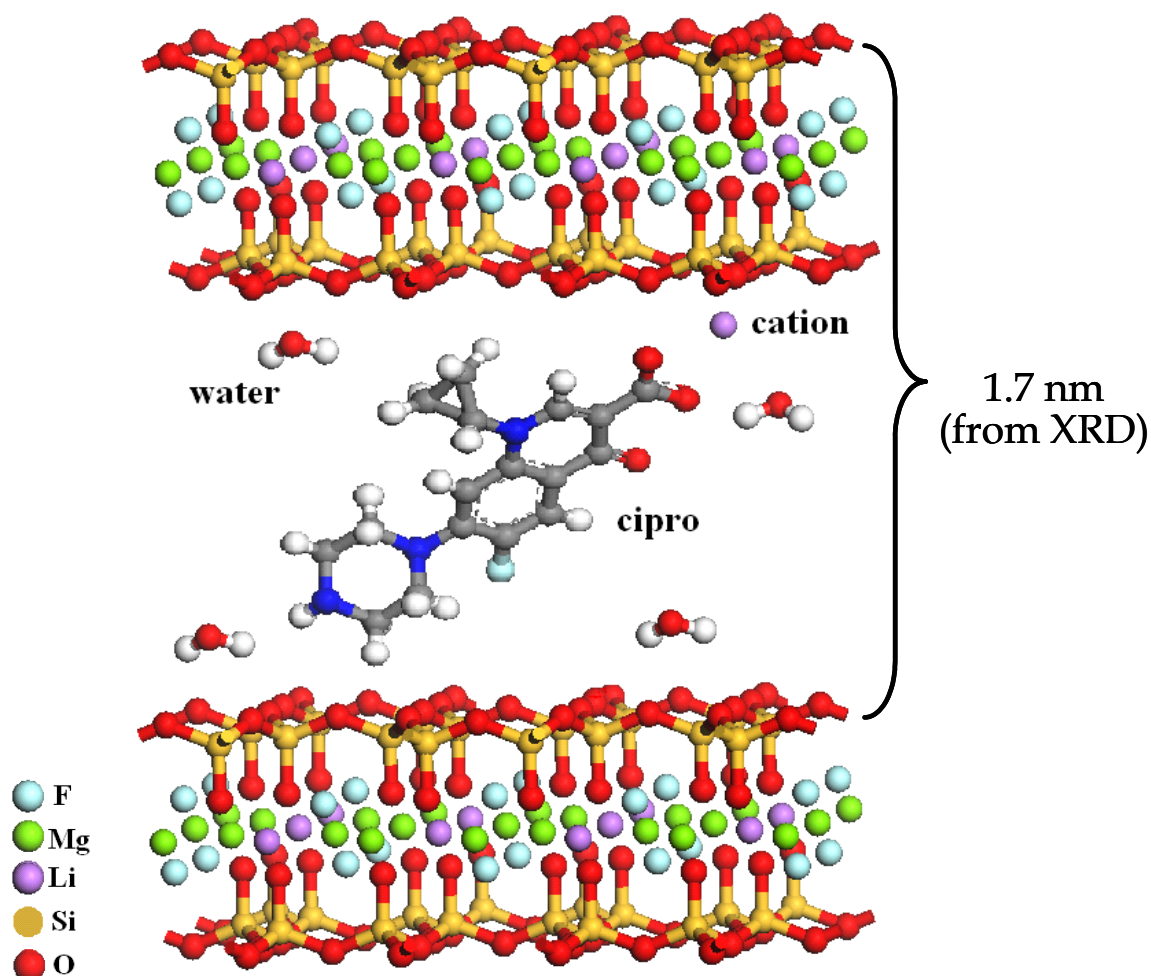


**Figure 3.** Sketch of the atomic structure of LiFh with intercalated Cipro.

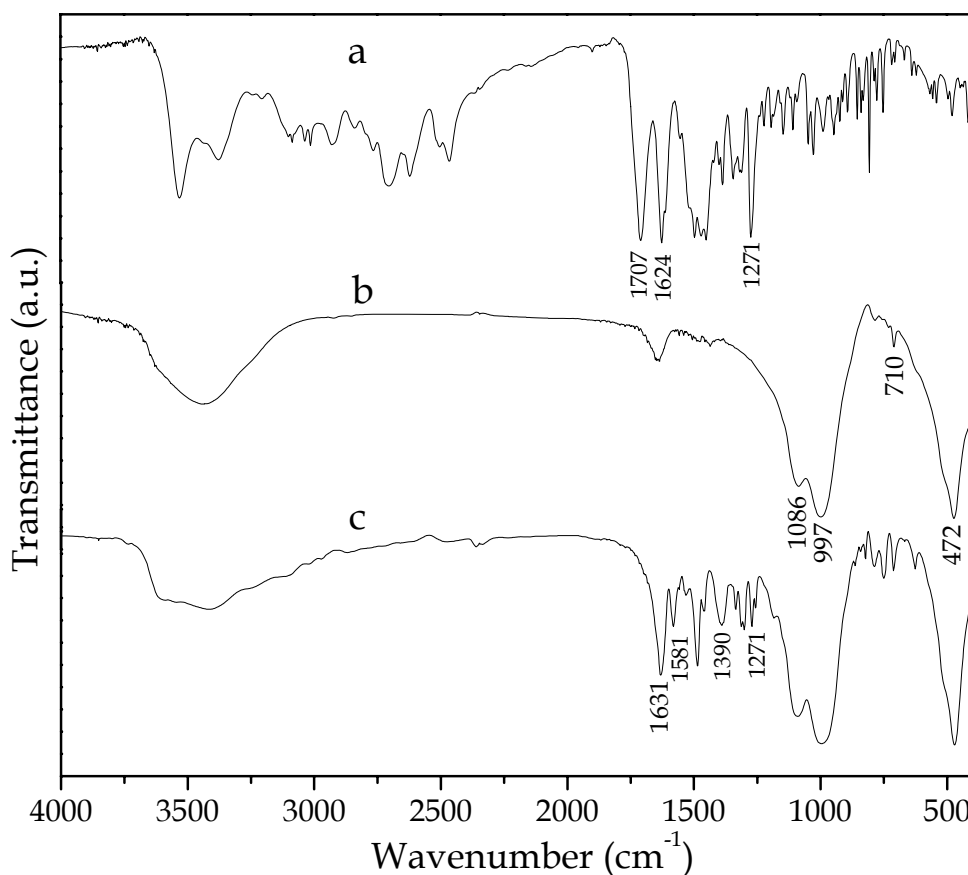


**Figure 4.** IR transmittance spectra for Cipro (a), LiFh (b), and composite LiFh-Cipro (c).

A more direct interaction between Cipro and clay was observed, as follows. A variation in the frequency of the band assigned to the Cipro from  $1624\text{ cm}^{-1}$  to  $1631\text{ cm}^{-1}$  after the interaction with the clay was also observed. The shift of this band in the LiFh-Cipro composite, as compared to the spectrum of Cipro alone, suggests strong interactions between the structures of Cipro and the clay via the ketone group. We do not see any evidence that the characteristic IR spectral bands of the clay are modified by the presence of Cipro in the composite.

Fig. 5 shows TG/DTG curves for Cipro, LiFh and LiFh-Cipro. The Cipro exhibits four main peaks of mass loss at 154, 299, 319 and 406. The Cipro decomposition is described as a sequence of three consecutive steps [28]: the first one is related to the loss of CO. The second one

occurs in the range 220–370 °C and is attributed to a loss of  $[C_4H_8N_2H_2 + CO]$  (two peaks in the DTG curve). The last one, above 370 °C, has been attributed to the removal of the residual drug as  $C_{11}H_8FNO$ . The DTG curve for the clay displays two important peaks attributed to desorption of water ( $\sim 100$  °C and  $\sim 150$  °C). The LiFh-Cipro composite shows peaks of mass loss in the region of 80 °C to 200 °C and approximately 350 °C. The peak around 350 °C can be assigned to the second step of the decomposition process of ciprofloxacin, which evidences its presence in the composite. When comparing the DTG curve of the Cipro with that of the LiFh-Cipro composite, it is observed that an increase takes place in the temperature of Cipro decomposition (at 299 and 319 °C) after the interaction with clay. Thus, its thermal stability is increased in the composite. The mass loss in the region 80 °C to 200 °C (last panel in Fig 5) could be attributed to the fact that water desorbs significantly easier from the composite than from the pure clay, which could be due to increased interlayer space when Cipro is intercalated.

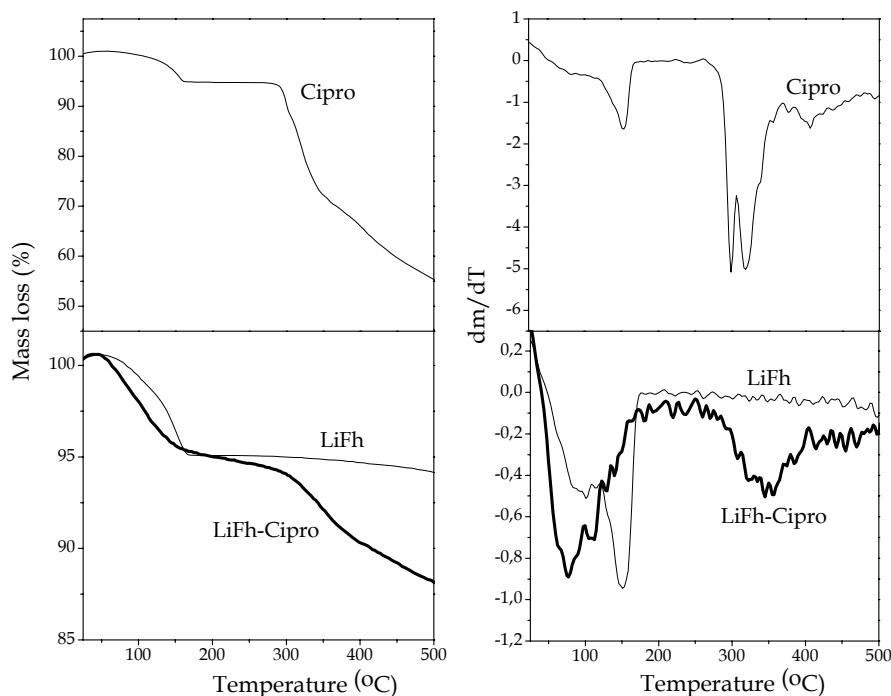


**Figure 5.** TG and differential thermogravimetry (DTG) curves for ciprofloxacin (Cipro), LiFh and composite LiFh-Cipro, at 10 °C/min.

### 3.3 Cipro release

Fig. 6 shows the percentage of Cipro released from the LiFh-Cipro colloidal suspension as a function of time at 37 °C and 65 °C. We observe that the Cipro amount released in SGJ increases as a function of time. At 37 °C and 65 °C the composite releases approximately up to 10 % and 25 % of the initial drug load (277 mg of Cipro per gram of clay; equivalent to 8.3 mg of Cipro per 30 mg of composite), respectively within 10 hours. This clearly demonstrates that the release dynamics of our composite is temperature-controlled, a potentially relevant feature for biomedical applications.

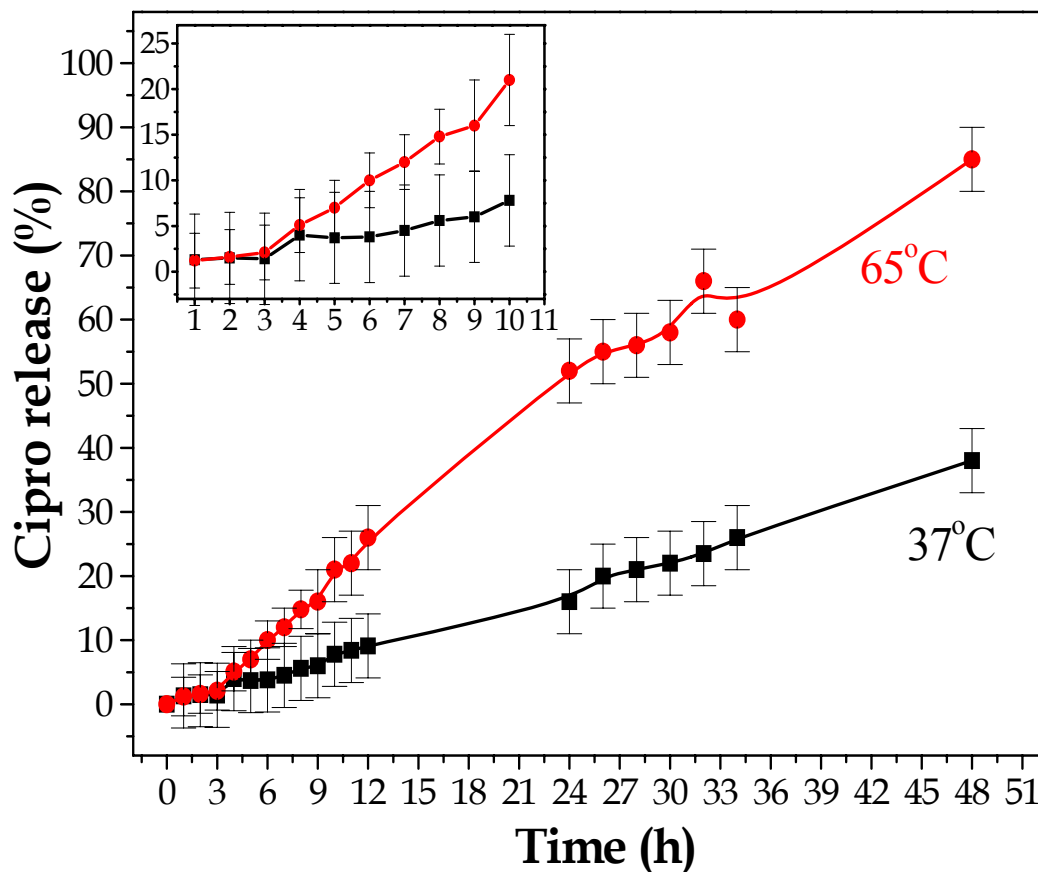


**Figure 6.** *In vitro* release curve of Cipro from a colloidal suspension of the composite LiFh-Cipro at 37°C and 65°C in synthetic gastric juice (SGJ).



The actual mechanism of drug capture by such smectite clay is not understood. We suggest three general alternative scenarios: One possibility could be that the Cipro molecule replaces the charge-compensating cations, in which case there would nominally be about 1.2 captured Cipro molecules associated with each unit cell of the clay. Another possibility is that the Cipro molecules do not replace the cations, but rather are attracted to the cations. So, in this case we can nominally associate a minimum of about 1.2 Cipro molecules per unit cell of the clay. Thirdly, and lastly we could imagine that the drug molecules are captured by the clay surfaces, and in this case there could be about at least 1 Cipro molecule associated with each unit cell, since the unit cell is the in-plane repetitive unit in the clay structure. In summary, whatever is the mechanism, it is reasonable to assume that approximately  $1.1 \pm 0.1$  Cipro molecules are captured per unit cell of the clay as a lower estimate for a clay fully loaded with drug molecules. The unit cell chemical formula for fluorohectorite is  $M_x(\text{Mg}_{6-x}\text{Li}_x)\text{F}_4\text{Si}_8\text{O}_{20}$ , where M denotes the exchangeable cations, giving a unit cell mass of about 754 (atomic mass units) for the clay, for  $M = \text{Li}$  and  $x \sim 1.2$ . The atomic mass of the Cipro molecule is about 368, which gives an estimate of the Cipro to clay mass ratio of about 368/754 for a compactly packed clay sample. Our clay samples typically have 40% mesoporosity [29], thus assuming about  $1.1 \pm 0.1$  Cipro molecules are captured per unit cell of the clay, we estimate the Cipro drug load to be approximately  $0.3 \pm 0.03$ . Our XRD and AAS characterization suggest that about 80 % of the mass of our powder samples is clay, and that the remaining 20% are impurities. Our UV results show that the Cipro mass incorporated per unit mass of sample is approximately 0.3, which translates into 0.35 of Cipro mass incorporated per unit mass of clay, if we assume that 20% of the impurities do not play a role in the capture of ciprofloxacin. This suggests that it is reasonable to assume that an important proportion of the Cipro is captured by the clay in the powder.

To understand the mechanisms involved, six standard models [30] applied to slow release systems were considered to describe the data. Within the error bars, our data can be well fitted by the zero order model [30].  $Q_t = Q_e + k_0t$  with  $Q_e = 0$  and  $k_0 = 0,76$  and  $1,93$  for  $37\text{ }^\circ\text{C}$  and  $65\text{ }^\circ\text{C}$ , respectively. This means that, for both temperatures the release follows an anomalous diffusion. This implies that the composite releases the same amount of drug per unit time, which is an ideal method of drug release for achieving sustained pharmacological action.

Figure 7 shows the percentage of ciprofloxacin released from the composite at 6 hours, as a function of temperature (here, we have just stopped the process at 6 h instead of the step-like aliquot collection associated to Figure 6). A clear increase in the slope of the curve is observed as temperature increases, confirming that the release in our system is temperature-controlled. The inset in figure 7 shows an Arrhenius thermal activation plot of the same data, giving an activation energy ( $E_a$ ) of approximately  $67\text{ kJ/mol}$  ( $0.7\text{ eV}$ ). The maximum release was observed at  $85\text{ }^\circ\text{C}$ , corresponding to 50% of the initial amount of ciprofloxacin.  $E_a$  can be viewed as the energy barrier a drug molecule must overcome to be released from the clay. Energies involved in physisorption are usually in the range of  $5\text{--}40\text{ kJ/mol}^{-1}$ , while activation energies from  $40$  to  $800\text{ kJ/mol}^{-1}$  are typical of chemisorptions [31,32]. Distinguishing between physical and chemical mechanisms is not always easy, in particular when the values of activation energies are near the limit between both phenomena. In the case of chemical adsorption, there is a direct chemical bond between the adsorbate and the surface; a chemically adsorbed molecule loses its identity on reaction or dissociation and cannot be recovered by desorption [33]. Physical adsorption does not involve any chemical bonds: the adsorbate is held by physical forces (i.e., van der Waals and electrostatic), it usually keeps its identity and, on desorption, returns to its original form. The value of  $E_a$  calculated from our Cipro desorption process is somewhat bigger than the lower limit typically used to define chemical adsorption ( $40\text{ kJ/mol}^{-1}$ ). This suggests a weak chemical

interaction mechanism, which is also supported by our IR spectroscopy results, where strong interactions between the Cipro structure and the clay via the ketone group may take place. However, our UV data after the interaction of the composite with synthetic gastric juice do not reveal any chemical interactions of the Cipro molecules with the clay. Finally, the slow release of Cipro in time suggests either a weak chemical interaction or a strong physical interaction. We are currently in time performing new experiments and computational simulations in order to shed light on the precise mechanisms involved in the incorporation and release of ciprofloxacin hydrochloride into/from clay fluorhectorite.

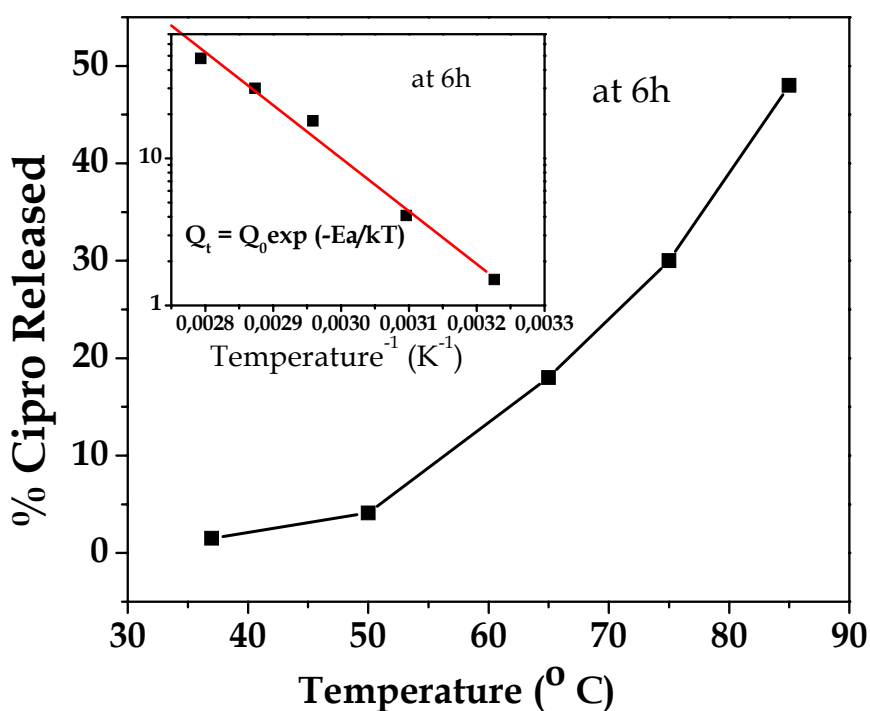


**Figure 7.** Percent of ciprofloxacin release from the composite LiFh-Cipro at different temperature and a fixed time in synthetic gastric juice (SGJ).

#### **4. Conclusion**

We have shown the ability of the clay Li-fluorohectorite to readily incorporate the antibiotic ciprofloxacin, up to 277 mg per gram of material. This amount will increase if the proportion of impurities in the host material is diminished. The incorporation takes place in the clay interlayer space, as demonstrated by XRD. *In vitro* release studies in colloidal suspensions of LiFh-Cipro show that the clay promotes the slow release of ciprofloxacin, and that the percentage of drug released increases both with time and with temperature. Thus, we have been able to produce a Temperature Controlled Release System (TCRS) with several potential biomedical applications.

We are currently working on the incorporation of other types of drugs. Future work will include experiments combined with simulations aimed to understanding the details of the capture and release mechanisms.

#### **Acknowledgments**

A. R. and L. Ch. M. thank the technical support from Pôle de Recherche et d'Enseignement Supérieur Sud de France (PRES). J. O. F., E. L. H. and Z. R. acknowledge support from the Research Council of Norway. E. A. and J. O. F. thank the Centre for Advanced Study at the Norwegian Academy of Science and Letters (CAS) under the project Complex Matter Science 2011-12. E.A. and A.R. acknowledge support by a TOTAL-ESPCI ParisTech Chair, and by PMMH/ESPCI. We thank Laboratorios MEDSOL for providing the pharmaceutical grade raw materials.

## References

- [1] J.-Y. Wu, S.-Q. Liua, P.W.-S. Heng, Y.-Y. Yanga, *J. Controlled Release* 102 (2005) 361.
- [2] G.D. Kang and S.C. Song, *Int. J. Pharm.* 349 (2008) 188.
- [3] D.C. Hyun, P. Lu, S.-I. Choi, U. Jeong, Y. Xia, *Angew. Chem. Int. Ed.* 52 (2013) 1.
- [4] A. Rivera and T. Farias, *Microporous Mesoporous Mater.* 80 (2005) 337.
- [5] G.V. Joshi, R.R. Pawar, B.D. Kevadiya, H.C. Bajaj, *Microporous Mesoporous Mater.* 142 (2011) 54.
- [6] J.K. Park, Y.B. Choy, J.-M. Oh, J.Y. Kim, S.-J. Hwang, J.-H. Choy, *Int. J. Pharm.* 359 (2008) 198–204.
- [7] G.V. Joshi, B.D. Kevadiya, H.A. Patel, H.C. Bajaj, R.V. Jasra, *Int. J. Pharm.* 374 (2009) 53.
- [8] A.R. Hamilton, G.A. Hutcheon, M. Roberts, E.E. Gaskell, *Appl. Clay Sci.* 87 (2014) 129.
- [9] T. Takahashi, Y. Yamada, K. Kataoka, Y. Nagasaki, *J. Control. Release* 107 (2005) 408.
- [10] E.L. Hansen, H. Hemmen, D.M. Fonseca, C. Coutant, K.D. Knudsen, T.S. Plivelic, D. Bonn, J.O. Fossum, *Sci. Rep. 2*, *Nature* (2012) 618.
- [11] H. Jung, H.M. Kim, Y.B. Choy, S.-J. Hwang, J.-H. Choy, *Int. J. Pharm.* 349 (2008) 283.
- [12] H.R. Bosshard, D.N. Marti, I. Jelesarov, *J. Mol. Recognit.* 17 (2004) 1.
- [13] M. Franchi, J.P. Ferris, E. Gallori, *Origins Life Evol. Biosphere* 33 (2003) 1.
- [14] G.J. da Silva, J.O. Fossum, E. DiMasi, K.J. Måløy, *Physical Review B* 67 (2003) 094114.
- [15] R.L. Anderson, I. Ratcliffe, H.C. Greenwell, P.A. Williams, S. Cliffe, P.V. Coveney, *Earth-Science Reviews* 98 (2010) 201.
- [16] P.D. Kaviratna, T.J. Pinnavaia, P.A. Schroder, *J. Phys. Chem. Solids* 57 (1996) 1897.
- [17] G. Løvoll, B. Sandnes, Y. Méheust, K.J. Måløy, J.O. Fossum, G.J. da Silva, M.S.P. Mundim, D.J. R., D.M. Fonseca, *Physica B* 370 (2005) 90.
- [18] United States Pharmacopeia, The United States Pharmacopeial Convention Inc., Rockville, MD, USP30-NF25 (2007).
- [19] P.C. Soares Jr., E.D. Zanotto, V.M. Fokin, H. Jain, *J. Non-Cryst. Solids* 331 (2003) 217.
- [20] H. Hemmen, L.R. Alme, J.O. Fossum, Y. Meheust, *Physical Review E* 82 (2010) 036315.
- [21] P. Komadel, J. Madejova, M. Janek, W.P. Gates, R.J. Kirkpatrick, J.W. Stucki, *Clays Clay Miner.* 44 (1996) 228.
- [22] C. Gu and K.G. Karthikeyan, *Environ. Sci. Technol.* 39 (2005) 9166.
- [23] P. Trivedi and D. Vasudevan, *Environ. Sci. Technol.* 41 (2007) 3153.
- [24] U. Neugebauer, A. Szeghalmi, M. Schmitt, W. Kiefer, J. Popp, U. Holzgrabe, *Spectrochim. Acta, Part A* 61 (2005) 1505.
- [25] I. Turel, P. Bukovec, M. Quirds, *Int. J. Pharm.* 152 (1997) 59.
- [26] J. Sun, S. Sakai, Y. Tauchi, Y. Deguchi, J. Chen, R. Zhang, K. Morimoto, *European Journal of Pharmaceutics and Biopharmaceutics* 54 (2002) 51.
- [27] W. Qingfeng, L. Zhaohui, H. Hanlie, *Journal of Wuhan University of Technology-Mater. Sci.* 27 (2012) 516.
- [28] N.E.A. El-Gamel, M.F. Hawash, M.A. M. A. Fahmey, *J. Therm. Anal. Calorim.* 108 (2012) 253.
- [29] K.D. Knudsen, J.O. Fossum, G. Helgesena, V. Bergaplass, *J. Appl. Crystallogr.* 36 (2003) 587.
- [30] I. Calabrese, G. Cavallaro, C. Scialabba, M. Licciardi, M. Merlic, L. Sciascia, M. Liria, M.L. Turco Liveri, *Int. J. Pharm.* 457 (2013) 224.

- [31] H. Nollet, M. Roels, P. Lutgen, P.V. der Meeren, W. Verstraete, *Chemosphere* 53 (2003) 655.
- [32] Y. Seki and K. Yurdakoç, *Adsorption* 12 (2006) 89.
- [33] J.-G. Choi, D.D. Do, H.D. Do, *Ind. Eng. Chem. Res.* 40 (2001) 4005.

**Smectite Clay as Ciprofloxacin delivery system:  
Intercalation and Temperature Controlled Release Properties**

**A. Rivera, L. Valdés, J. Jiménez, I. Pérez, A. Lam, E. Altshuler, L. C. de Ménorval,  
J. O. Fossum, E. L. Hansen, Z. Rozynek**

**Figure Captions**

Figure 1. Representation of the atomic (a) and molecular structure (b) of the LiFh clay and ciprofloxacin drug, respectively.

Figure 2. Diffraction patterns for LiFh and LiFh-Cipro composite.

Figure 3. Sketch of the atomic structure of LiFh with intercalated Cipro.

Figure 4. IR transmittance spectra for Cipro (a), LiFh (b), and composite LiFh-Cipro (c).

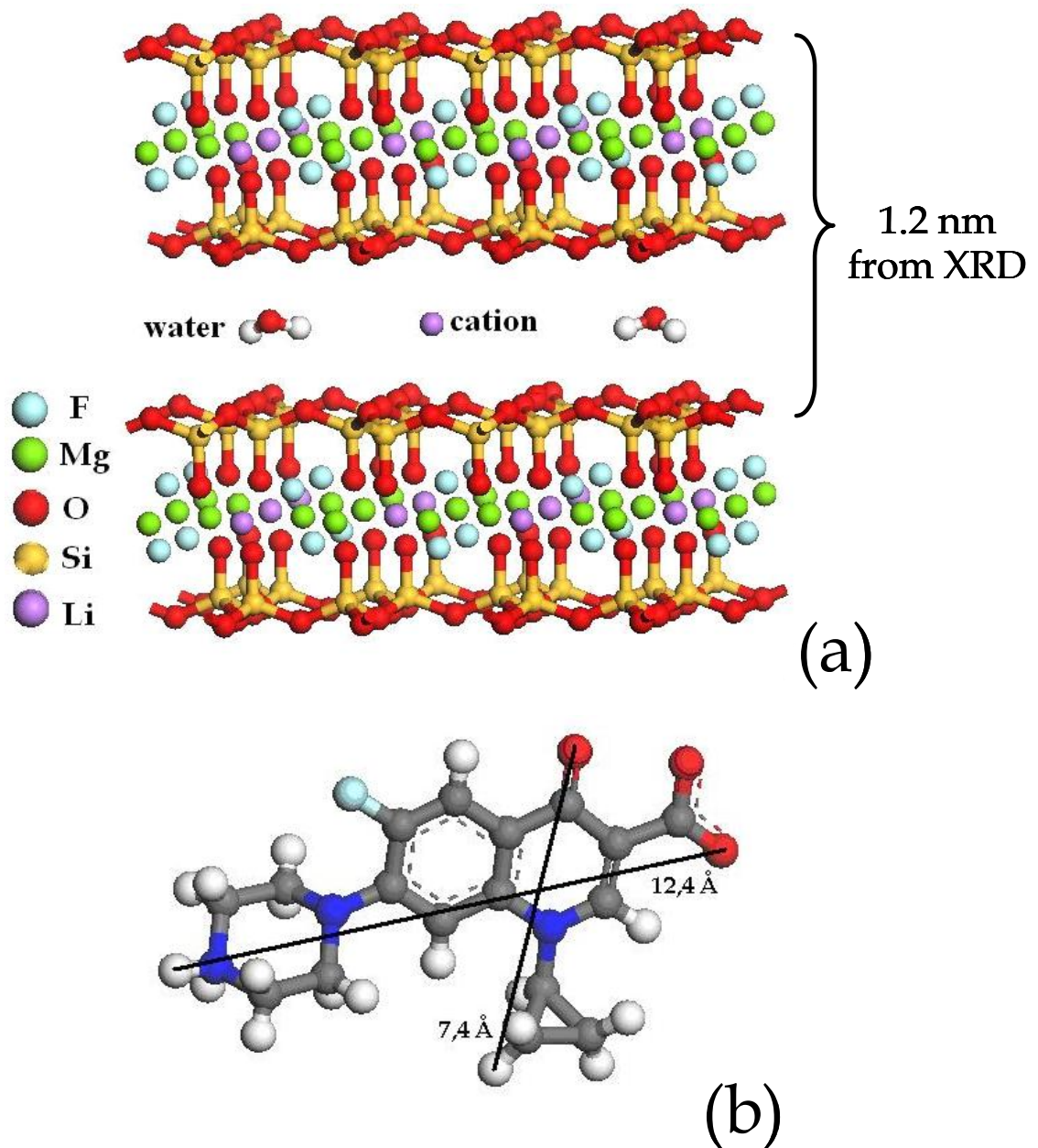
Figure 5. TG and differential thermogravimetry (DTG) curves for ciprofloxacin (Cipro), LiFh and composite LiFh-Cipro, at 10 °C/min.

Figure 6. *In vitro* release curve of Cipro from the composite LiFh-Cipro at 37°C and 65°C in synthetic gastric juice (SGJ).

Figure 7. Percent of ciprofloxacin release from the composite LiFh-Cipro at different temperature and a fixed time in synthetic gastric juice (SGJ).

**Smectite Clay as Ciprofloxacin Delivery System:  
Intercalation and Temperature Controlled Release Properties**

**A. Rivera, L. Valdés, J. Jiménez, I. Pérez, A. Lam, E. Altshuler, L. C. de Ménorval,  
J. O. Fossum, E. L. Hansen, Z. Rozynek**



**Figure 1.** Schematic representation of the atomic (a) and molecular structure (b) of the LiFh clay and ciprofloxacin drug, respectively.



**Smectite Clay as Ciprofloxacin Delivery System:  
Intercalation and Temperature Controlled Release Properties**

**A. Rivera, L. Valdés, J. Jiménez, I. Pérez, A. Lam, E. Altshuler, L. C. de Ménorval,  
J. O. Fossum, E. L. Hansen, Z. Rozynek**

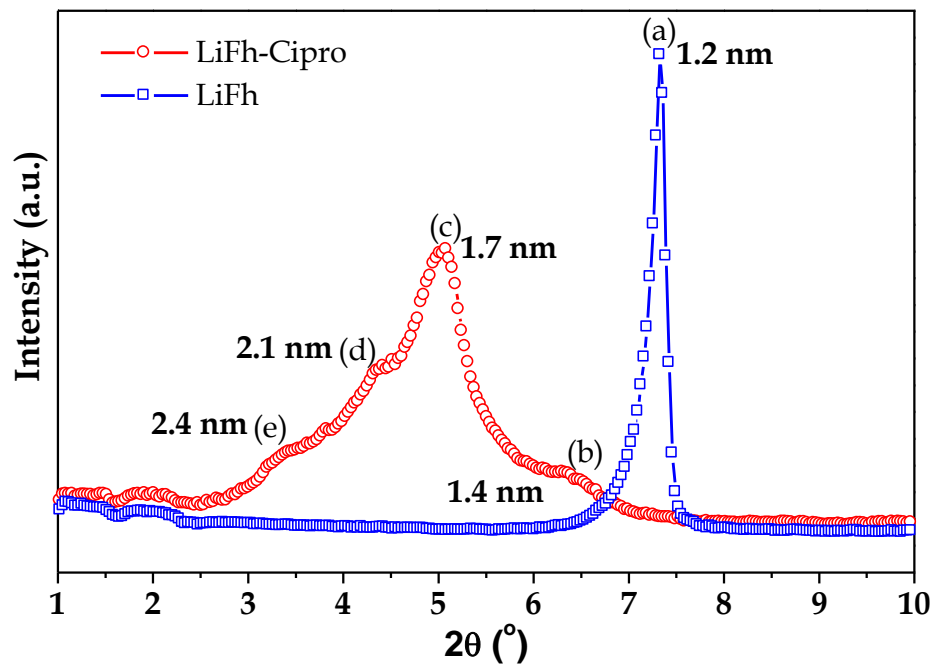


**Figure 2.** Diffraction patterns for LiFh and LiFh-Cipro composite.

**Smectite Clay as Ciprofloxacin Delivery System:  
Intercalation and Temperature Controlled Release Properties**

**A. Rivera, L. Valdés, J. Jiménez, I. Pérez, A. Lam, E. Altshuler, L. C. de Ménorval,  
J. O. Fossum, E. L. Hansen, Z. Rozynek**

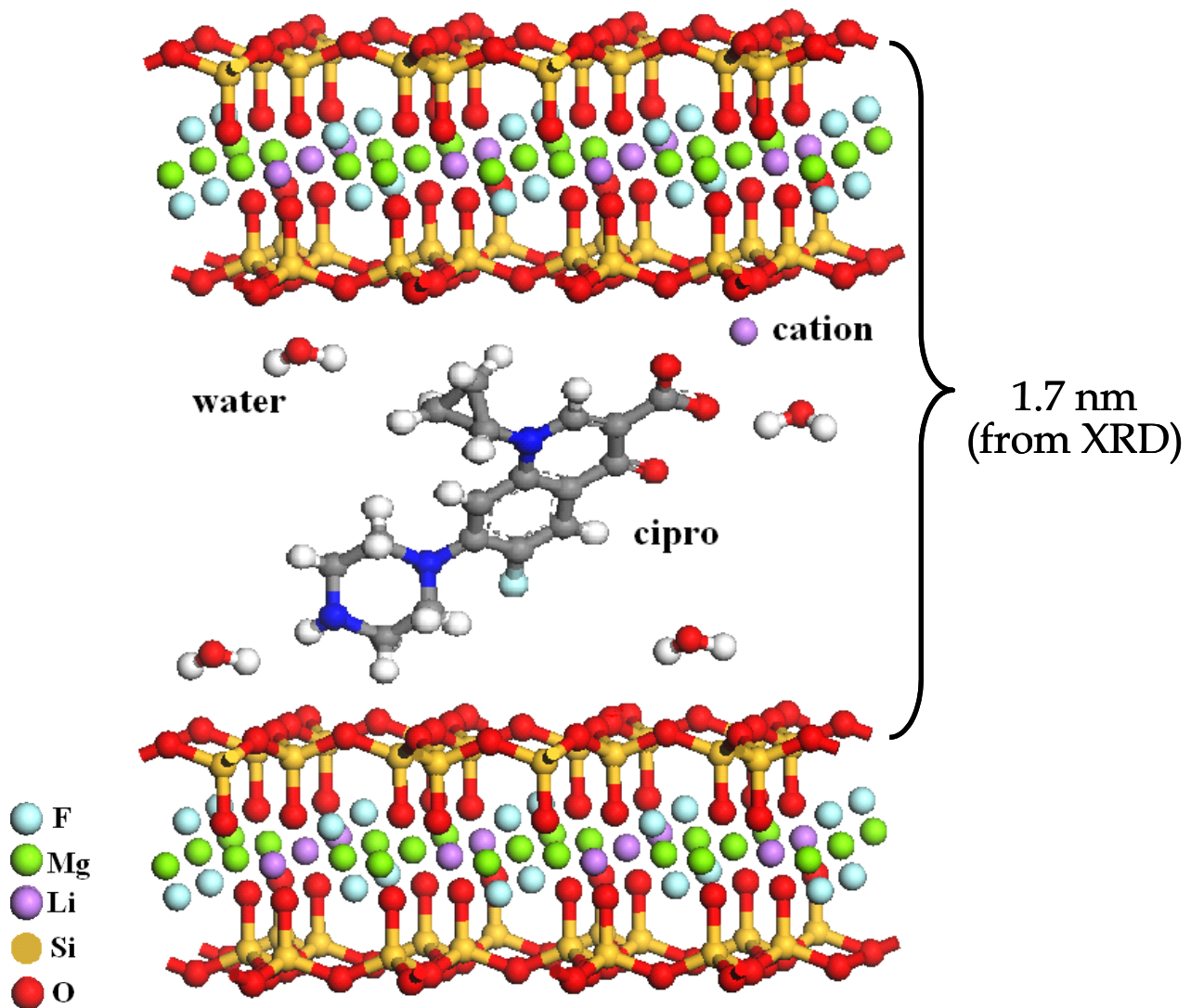


**Figure 3.** Sketch of the atomic structure of LiFh with intercalated Cipro.

**Smectite Clay as Ciprofloxacin Delivery System:  
Intercalation and Temperature Controlled Release Properties**

**A. Rivera, L. Valdés, J. Jiménez, I. Pérez, A. Lam, E. Altshuler, L. C. de Ménorval,  
J. O. Fossum, E. L. Hansen, Z. Rozynek**

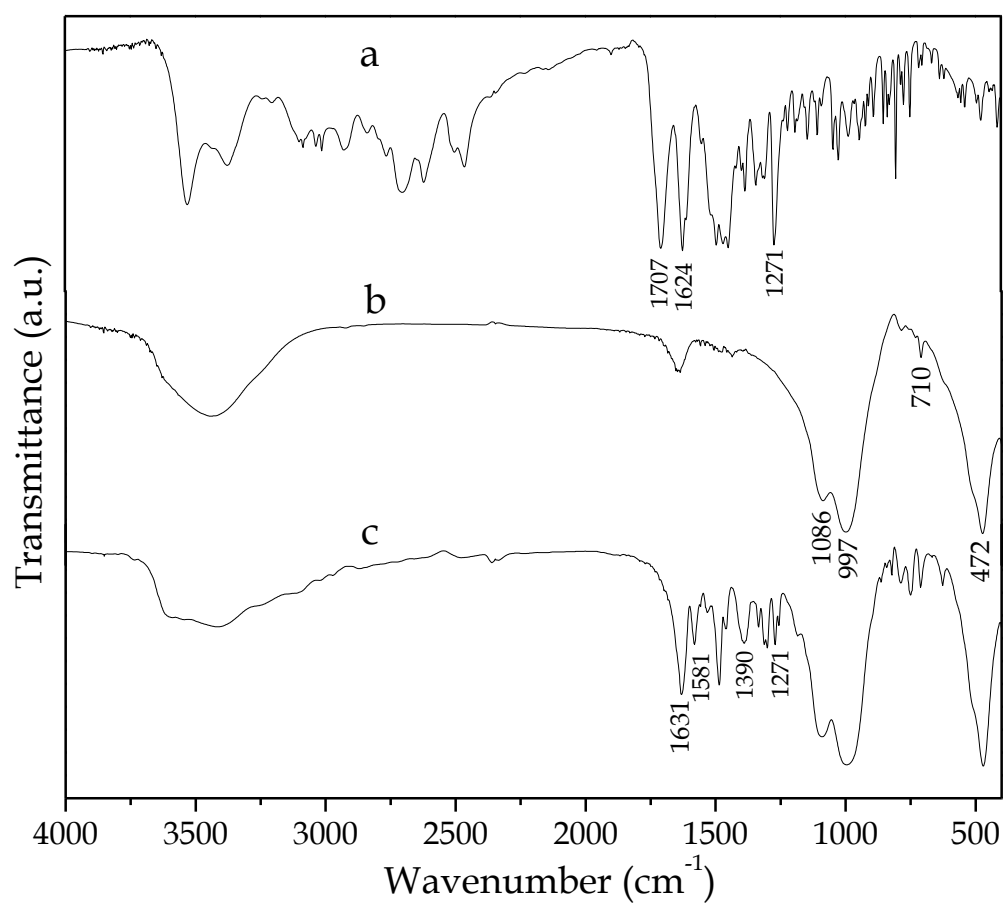


**Figure 4.** IR transmittance spectra for Cipro (a), LiFh (b), and composite LiFh-Cipro (c).

**Smectite Clay as Ciprofloxacin Delivery System:  
Intercalation and Temperature Controlled Release Properties**

**A. Rivera, L. Valdés, J. Jiménez, I. Pérez, A. Lam, E. Altshuler, L. C. de Ménorval,  
J. O. Fossum, E. L. Hansen, Z. Rozynek**

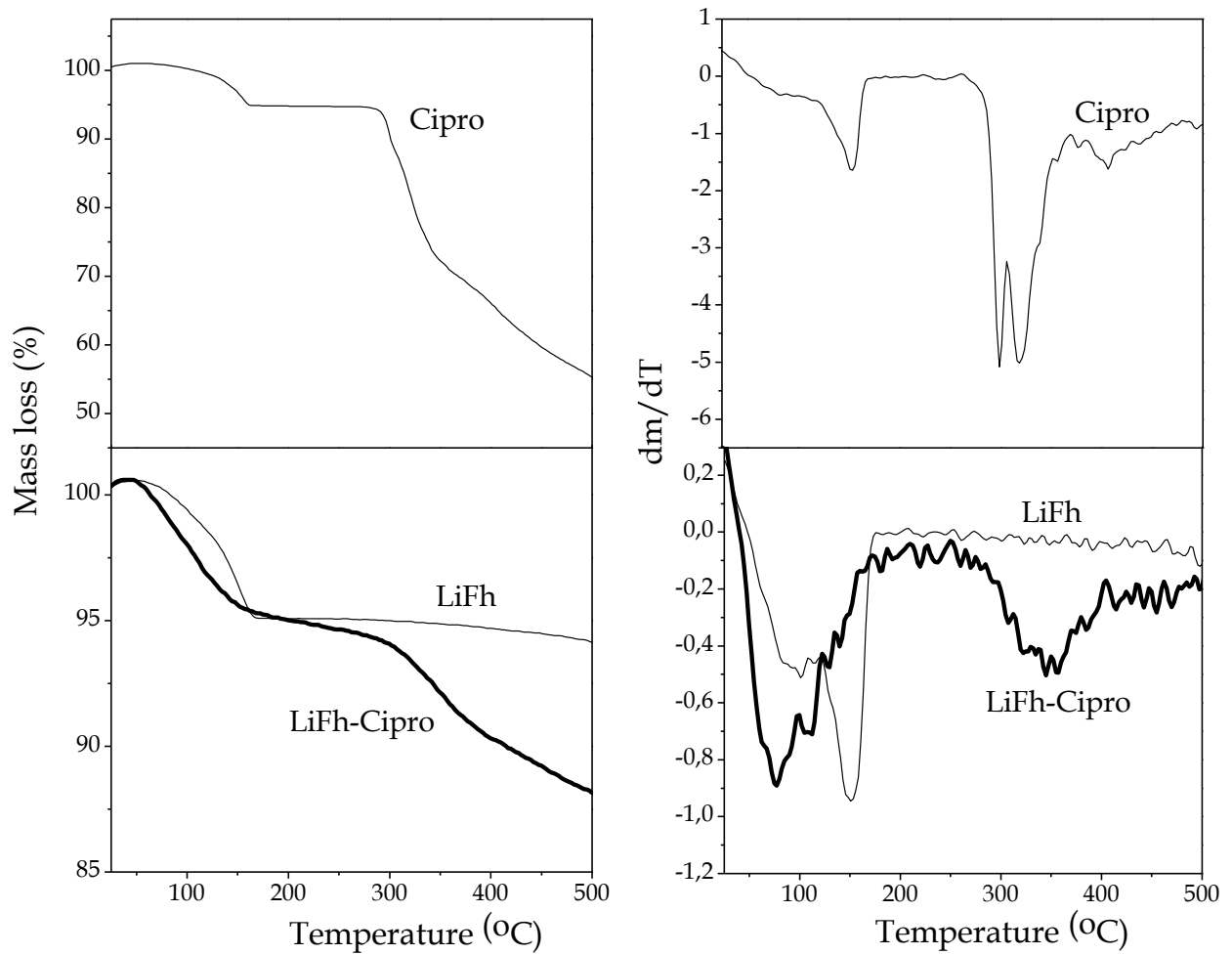


**Figure 5.** TG and differential thermogravimetry (DTG) curves for ciprofloxacin (Cipro), LiFh and composite LiFh-Cipro, at 10 °C/min.

**Smectite Clay as Ciprofloxacin Delivery System:  
Intercalation and Temperature Controlled Release Properties**

**A. Rivera, L. Valdés, J. Jiménez, I. Pérez, A. Lam, E. Altshuler, L. C. de Ménorval,  
J. O. Fossum, E. L. Hansen, Z. Rozynek**

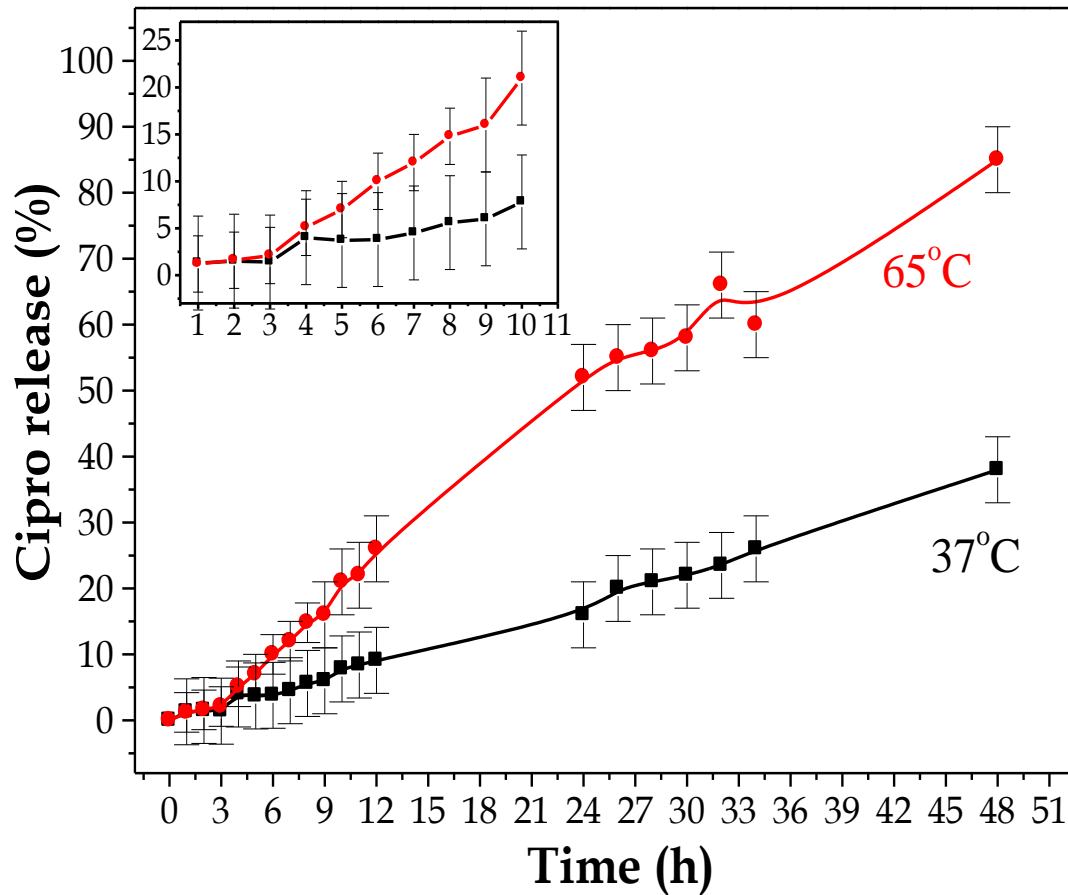


**Figure 6.** *In vitro* release curve of Cipro from a colloidal suspension of the composite LiFh-Cipro at 37°C and 65°C in synthetic gastric juice (SGJ).

**Smectite Clay as Ciprofloxacin Delivery System:  
Intercalation and Temperature Controlled Release Properties**

A. Rivera, L. Valdés, J. Jiménez, I. Pérez, A. Lam, E. Altshuler, L. C. de Ménorval,  
J. O. Fossum, E. L. Hansen, Z. Rozynek

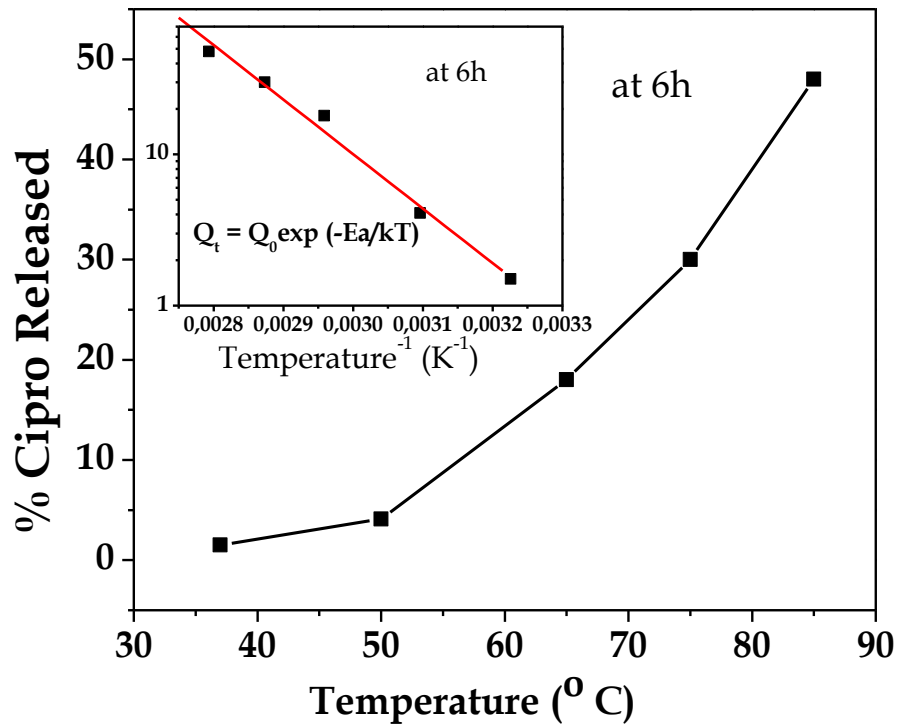


**Figure 7.** Percent of ciprofloxacin release from the composite LiFh-Cipro at different temperature and a fixed time in synthetic gastric juice (SGJ).